Computational simulation of nuclear medicine images in patients with thyroid diseases

María Julia Vitaller[1], Enzo Aman[2], José Luis De la Cruz Marin[3], Venecia Magalí Calandrón[4], Cecilia Yamil Chain[5] and Luis Héctor Illanes [6]

[1] 0009-0007-0544-8487, INIFTA (UNLP CONICET), La Plata, Argentina
[2] 0009-0002-8561-0547, Facultad de Ciencias Exactas, UNLP, La Plata, Argentina
[3] 0000-0003-1490-5196, IREN Centro, Concepción, Perú; UNMSM, Lima, Perú
[4] 0009-0003-4944-8375, Facultad de Ciencias Exactas, UNLP, La Plata, Argentina
[5] 0000-0002-8234-0556, INIFTA (UNLP CONICET), La Plata, Argentina
[6] 0000-0003-1432-7752, Facultad de Ciencias Exactas, UNLP, La Plata, Argentina

mjvitaller@inifta.unlp.edu.ar, enzo.aman@fisica.unlp.edu.ar, jose.delacruz.m@uni.pe, venecia.calandron@fisica.unlp.edu.ar, yamil@inifta.unlp.edu.ar, luis.illanes@fisica.unlp.edu.ar

Abstract. The aim of modeling and simulation was to predict the accuracy of the quantitative data that can be extracted from NM images obtained with the medical equipment available in our setting. The simulation model was based on two existing tools: the SIMIND Monte Carlo code, which models a clinical scintillation camera for acquiring both planar and tomographic NM images, and a voxelized anthropomorphic computational Zubal phantom as an anatomical model of the patient with a thyroid disease. The results showed that the possibility of quantification depends on the depth of the anatomical structure that incorporates the radioiodine and on the imaging modality. The knowledge of the accuracy of quantification from the NM can contribute to personalizing radiopharmaceutical treatments.

Keywords: SIMIND Montecarlo, Zubal phantom, SPECT, thyroid planar images, activity quantification.

Simulaciones computacionales de imágenes de Medicina Nuclear en pacientes con enfermedades tiroideas

Resumen. El objetivo del modelado y la simulación fue predecir la exactitud de la información cuantitativa que puede ser extraída de las imágenes de MN obtenidas con el equipo médico disponible en nuestro entorno. El modelo de simulación se basó en dos herramientas existentes: el código Monte Carlo SIMIND, que modela una cámara de centelleo clínica para adquirir imágenes de MN tanto planares como tomográficas, y un fantoma computacional antropomórfico voxelizado Zubal como modelo anatómico de pacientes con enfermedad tiroidea. Los resultados mostraron que la precisión de la cuantificación depende de la profundidad de la estructura anatómica que incorpora el radioyodo y de la modalidad de imagen. El conocimiento de la exactitud de cuantificación de las imágenes de MN puede contribuir a la personalización de los tratamientos con radiofármacos.

Palabras clave: SIMIND Montecarlo, fantoma Zubal, SPECT, imágenes planares de tiroides, cuantificación de actividad.

1 Introduction

Nuclear Medicine (NM) imaging involves the detection of the biodistribution of a radioactive material, called radiopharmaceutical, and has historically contributed with semi- quantitative information to medical diagnosis (Illanes et al., 2022) using gamma cameras and Single Photon Emission Computed Tomographers (SPECT). An important milestone to advance toward personalized NM is optimization of radiopharmaceutical use in clinical practice, that involves the quantification of the radioactive material from the NM images. Nevertheless, the sophisticated quantitative instruments are not available in most of the healthcare centers of our region. Modeling and computational simulation provide a controlled environment for evaluating the performance and limitations of imaging systems, particularly for activity quantification tasks, where direct experimental assessment may be limited by physical and clinical constraints.

In this work we model and simulate the acquisition of gamma camera and SPECT images in patients with thyroid diseases with the aim to predict the accuracy of extracting quantitative data from the images that are acquired with real medical equipment.

2 Computational tools and methodologies

Three case studies are presented, by combining different imaging modalities and different thyroid diseases clinical profiles (Vitaller, 2025, De la Cruz Marin et al, 2025; Calandrón, 2026). The modelling and simulation were performed using a 32 GB RAM, 512 GB SSD Laptop with i7-uu85g7 processor.

2.1 SIMIND Monte Carlo modeling of a clinical scintillation camera

SIMIND Monte Carlo code (Ljungberg, 2022) was used to create two virtual clinical simulators, defining all detector parameters according to the Picker Prism 2000 XP gamma camera and the General Electric Discovery NN 360 SPECT instrument specification sheets, with a 0.95 cm crystal thickness and a high- energy collimator. The simulators were subjected to the routine quality control (QC) tests intrinsic uniformity (UFOV, CFOV) and extrinsic resolution under identical conditions used in the clinic (NEMA, 2017).

2.2 Zubal anthropomorphic phantom as anatomical model of the patient

The Zubal phantom (Zubal et al., 1994) was modified to model the biodistribution of the radiopharmaceutical [^{131}I] sodium iodide that is observed in patients with thyroid diseases. A known amount of radioactivity (acting as ground truth for the simulations) was inserted in two different sized spheres mimicking tumors (from here on referred as thyroid remnant and lung metastases in the malignant disease) and in the thyroid gland of the phantom (benign disease).

2.3 Activity quantification in the simulated images

Simulated images, acquired with the virtual scintillation cameras in the modeled patients were analyzed using Fiji software to obtain the counts in the regions of interests (ROIs). With the aim of inferring the activity associated with the counts, a calibration source with a known ratio counts/MBq was included in the phantom. In the case of malignant thyroid disease planar images, further attenuation corrections in the obtained activity were done based on the Conjugate View Method (CVM) (Jönsson et al., 2005).

The quantified activities (A_S) were compared with the corresponding ground-truth activities (A_P) and the accuracy in the activity quantification was calculated as:

$$\textit{Relative Percentage Error (RPE)}=100\ (A_S - A_P)/\ A_P \qquad (1)$$

3 Results

3.1 Validation of the virtual clinical simulators

Table 1 shows the QC results obtained with virtual clinical simulators, that are consistent with the QC values expected by the manufacturers of the real gamma cameras (NEMA, 2007; GH Healthcare, 2018) validating the modelized clinical simulators.

Table 1. QC results for the virtual clinical simulators and for the real instruments

Simulated instrument	QC test	Simulated value	Expected value
Picker Prism 2000 XP	UFOV	2.66 %	≤ 5 %
	CFOV	2.36 %	2- 3%
	Extrinsic Resolution	1.52 cm	1.20 cm
GE Discovery 360 NM	UFOV	2.40 %	2.30 %
	CFOV	2.22 %	2.23 %
	Extrinsic Resolution	0.99 cm	1.09 cm

3.2 Simulated planar and tomographic NM images

The simulated planar anterior view (AV) of the malignant (Fig, 1.1) and benign (Fig. 1.2) thyroid disease and transversal views of the SPECT image of the malignant thyroid disease (Fig. 1.3A and 3B) verified that the distribution of the activity is consistent with the location of the tumoral lesions and, in the case of thyroid, with the butterfly- shape of the gland, confirming that the simulated images exhibit the same features of real clinical images.

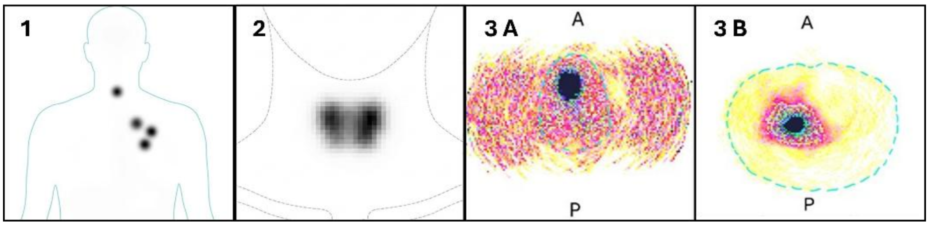

Fig. 1. Simulated planar and SPECT images: (1) Thyroid remnants and metastatic lesions, (2) Hyperthyroidic thyroid. (3) Transversal view of a SPECT image of a thyroid remnant (3A) and a metastatic lesion (3B). (A: anterior, P: posterior). The external contouring of the body is included, with the aim of interpreting the image.

3.3 Activity quantification in the simulated images

In Table 2, the ground- truth activity in the different anatomical structures, the quantified activity in the same structures obtained from the simulated images and the accuracy in the activity quantification (equation 1) are presented.

Table 2. Accuracy in the quantification of radiopharmaceutical activity from NM images of patients with malignant and benign thyroid pathologies

Simulated instrument	Modeled thyroid disease	Anatomical structure	Ground- truth activity [MBq]	Quantified activity [MBq]	RPE [%]
Picker Prism 2000 XP gamma camera	Malignant	Thyroid remnant	8.74	8.25	- 5.45
		Lung metastasis	145	127.55	-12.03
	Benign	Thyroid	2.50	2.56	2.40
GE Discovery 360 NM	Malignant	Thyroid remnant	550	331.64	-40.91
		Lung metastasis	74	44.44	-39.94

The activity that is quantified from the simulated images is, in general, smaller than the ground truth activity of the anatomical structure, meaning that not all the radioactive emissions that are produced are detected by the gamma camera. This finding is related to the attenuation of the photons in the patient's body, that limits the amount of radiation that interacts with the detector.

The best accuracy in the quantification of the activity is obtained from the planar image of the hyperthyroidic thyroid, fact that is ascribed to the very superficial position of the gland in the neck, that permits that virtually all the emitted radiation interacts with the detectors. In the case of small and deep structures, like thyroid remnants and lung metastases, the activity quantification from planar images using the CVM is more accurate than the quantification from SPECT images, as CVM considers correction for the deleterious effect of attenuation, diminishing the error in a factor of 4-7.

4 Conclusions

We modeled and simulated the acquisition of NM gamma camera and SPECT images in patients with malign and benign thyroid diseases. From a clinical perspective, our results suggested that in cases of patients with small tumoral lesions, it would be preferable to quantify from planar images using the CVM method than to rely on SPECT images for the quantification. In benign thyroid disease, the anatomical position of the gland allows an accurate quantification using the AV planar image.

From a computational perspective, this approach provides a framework for evaluating the performance and limitations of NM imaging systems under controlled conditions, contributing to the implementation of personalized NM therapies.

References

Calandrón, V. M. (2026). Utilidad de las simulaciones basadas en Montecarlo para implementación de cálculos dosimétricos en tratamientos de hipertiroidismo (Doctoral dissertation, Universidad Nacional de La Plata).

De la Cruz Marin, J. L., Chain, C. Y., & Illanes, L. H. (2025, June). Modelo computacional de una cámara gama como simulador de imágenes clínicas. In *Anales (Asociación Física Argentina)* (Vol. 36, No. 2, pp. 1-1). Asociación Física Argentina.

GH Healthcare Technical Publications. NM General Pur pose 600/800 Series*.DICOM CONFORMANCE STATE MENT revision 15. 2018. https://www.gehealthcare.com/-/jssmedia/349cb2b11ff043d7a8c7ea4d2cca150f.pdf?la=fr-ca

Illanes, L. H., Chain, C. Y., & Sánchez, J. (2022). *Simulaciones computacionales en medicina nuclear*. *Libros de Cátedra*. EDULP (Editorial de la Universidad Nacional de La Plata).

Jönsson, L., Ljungberg, M., & Strand, S. E. (2005). Evaluation of accuracy in activity calculations for the conjugate view method from Monte Carlo simulated scintillation camera images using experimental data in an anthropomorphic phantom. *Journal of Nuclear Medicine*, *46*(10), 1679-1686.

Ljungberg, M. (Ed.). (2022). *Handbook of Nuclear Medicine and Molecular Imaging for Physicists: Instrumentation and Imaging Procedures, Volume I*. CRC Press.

National Electrical Manufacturers Association (NEMA), 2007. Standards Publication NU 1-2007: Performance Measurements of Gamma Cameras. NEMA, Rosslyn, VA.

Vitaller, M. J. (2025). *Evaluación de métodos de cuantificación de actividad de 131 I a partir de imágenes bidimensionales: Análisis comparativo utilizando SIMIND MC* (Doctoral dissertation, Universidad Nacional de La Plata).

Zubal, I. G., Harrell, C. R., Smith, E. O., Rattner, Z., Gindi, G., & Hoffer, P. B. (1994). Computerized three-dimensional segmented human anatomy. *Medical physics*, *21*(2), 299-302.